Dynamics of N_2O decomposition over HZSM-5 with low Fe content

Dmitri A. Bulushev, Lioubov Kiwi-Minsker,* and Albert Renken

Swiss Federal Institute of Technology, LGRC-EPFL, CH-1015 Lausanne, Switzerland

Abstract

The dynamics of N_2O decomposition to gaseous nitrogen and oxygen over HZSM-5 catalysts with a low iron content (200 and 1000 ppm) was studied by the transient response method in the temperature range 523–653 K. The active catalysts were prepared from HZSM-5 with Fe in the framework on its steaming at 823 K followed by thermal activation in He at 1323 K. Two main steps were distinguished in the dynamics of N_2O decomposition. The first step represents N_2O decomposition forming gaseous nitrogen and surface atomic oxygen. The second step is associated with surface oxygen recombination and desorption. At 523–553 K only the first step is observed. Above 573 K the decomposition of N_2O to O_2 and N_2 in stoichiometric amounts starts at a rate increasing with time until a steady-state value is reached. This increase was assigned to the catalysis by adsorbed NO formed slowly on the catalyst surface from N_2O, as indicated by temperature-programmed desorption. The catalytic effect of the adsorbed NO was also confirmed by transient experiments with forced addition of NO in the stream of N_2O during its decomposition. A simplified kinetic model is proposed to explain the autocatalytic reaction. Catalyst pretreatment in O_2 did not affect N_2O decomposition, but irreversible water vapor adsorption at 603 K resulted in a twofold decrease in surface oxygen loading from N_2O and complete inhibition of the oxygen desorption.
© 2003 Elsevier Inc. All rights reserved.

Keywords: Fe-containing HZSM-5; N_2O decomposition; Transient response method; Temperature-programmed desorption; Surface oxygen loading from N_2O

1. Introduction

N_2O is a greenhouse gas with a warming potential 310 times higher than that of CO_2, and its concentration in the atmosphere is still on the rise [1]. Metal- and metal oxide-doped zeolites have been reported as promising catalysts for N_2O decomposition [2]. HZSM-5 with a low content of iron (hereafter H(Fe)ZSM-5) was shown to be active in nitrous oxide decomposition, forming surface atomic oxygen $(O)_{ad}$ and gaseous N_2 and O_2 [3]. The sites in H(Fe)ZSM-5 active in the above-mentioned processes have been assigned to iron cations [3–6]. But until now very little quantitative information has been available on the total loading of $(O)_{ad}$ and its role during N_2O decomposition to O_2 and N_2. Moreover, H(Fe)ZSM-5 is able to hydroxylate benzene to phenol and oxidize methane to methoxy species by N_2O at low temperatures [7,8]. For these reactions, N_2O decomposition to gaseous oxygen and nitrogen is a side reac-

tion decreasing the concentration of the reactant [9], which should be avoided.

The kinetics of N_2O decomposition was shown to be of first order in N_2O concentration [4]. The activity of zeolites in N_2O decomposition is known to depend on the presence of NO_x, O_2, H_2O, SO_2, CO, and hydrocarbons in streams. El-Malki et al. [4,10] and Zhu et al. [5] did not find any effect of oxygen on this reaction, but in the presence of water vapor, isothermal oscillations were observed during N_2O decomposition with Fe/MFI [4,10]. Perez-Ramirez et al. [6,11] studied the effect of NO on N_2O decomposition and showed that oxygen desorption is the rate-limiting step, which could be accelerated by NO. The objective of the present study was to determine the effect of O_2, NO, and H_2O on the dynamics of N_2O decomposition over H(Fe)ZSM-5. The transient response method gives valuable information concerning reaction dynamics and the effect of different gases. This method was applied earlier to study N_2O decomposition over Cu-ZSM-5 catalysts [12] and may shed additional light on the mechanism of the reaction over H(Fe)ZSM-5. In our previous study [13] it was shown that the transient response method allows determination of the concentration of

---

Fe sites active in the formation of surface atomic oxygen via N_2O decomposition to gaseous N_2 and $(O)_{ad}$.

2. Experimental

In our previous study [13] it was found that thermal pretreatment of steamed zeolites in He at 1323 K increases the concentration of sites active in N_2O decomposition, which were assigned to surface Fe-containing species. Therefore, this treatment was used during this study. Zeolites with very small concentrations of iron ($\leqslant 1000$ ppm) were employed, aiming at the formation of uniform Fe species. Low temperatures were used to study N_2O decomposition to discriminate between the different reaction steps.

2.1. Synthesis of catalysts

Two zeolites, HZSM-5$_{1000Fe}$ and HZSM-5$_{200Fe}$, were used throughout this study. The initial parent HZSM-5$_{1000Fe}$ (Zeocat PZ-2/50-H) with a Si/Al ratio of 25 and specific surface area (SSA) of 335 m^2/g was provided by Chemie Uetikon SA (Switzerland). The initial parent HZSM-5$_{200Fe}$ with a Si/Al ratio of 42 and SSA of 370 m^2/g was synthesized as reported elsewhere [13]. The synthesis solution was prepared from sodium aluminate (52.5 wt% $NaAlO_2$, Riedel–de Haën), sodium chloride (99.5 wt%, Fluka), and tetrapropylammonium hydroxide (20 wt% in water, Fluka) in deionized water by adding the tetraethyl orthosilicate (TEOS, 98%, Merck–Suchardt) with vigorous stirring (2–3 h). The molar ratio was as follows: TPA-OH:$Si(OEt)_4$:NaCl:$NaAlO_2$:H_2O = 2.16:5.62:3.43:0.13:1000. The synthesis took 2 days under an autogenously regulated pressure at 444 K. After being washed and calcined at 873 K in air for 5 h, the zeolite was converted into H form using ammonia buffer, and heated in nitrogen at 823 K for 5 h. For activation the zeolites were steamed (H_2O partial pressure was 310 mbar) in a N_2 flow for 3 h at 823 K and treated in He for 4 h at 1323 K. This treatment did not alter zeolite structure as was shown by X-ray diffraction (XRD) of the zeolites before and after activation.

2.2. Catalyst characterization

Fe and Al content of the catalysts was measured by atomic absorption spectroscopy (AAS) using a Shimadzu AA-6650 spectrophotometer with an air–acetylene flame.

XRD patterns of the catalysts were obtained with a Siemens D500 diffractometer with Cu-K_α monochromatic radiation ($\lambda = 1.5406$ Å). XRD of the HZSM-5$_{200Fe}$ catalyst after activation by steaming following severe high-temperature treatment in He (1323 K, 17 h) showed only peaks corresponding to HZSM-5.

The specific surface area of the catalysts was determined using N_2 adsorption–desorption at 77 K with a Sorptomatic 1990 instrument (Carlo Erba). The SSA of the samples was calculated employing the BET method. The SSA of HZSM-5$_{200Fe}$ catalyst decreased after activation, but not substantially (from 370 to 330 m^2/g).

2.3. Catalytic activity measurements

Catalytic activity was measured in a Micromeritics AutoChem 2910 analyzer. A ThermoStar 200 (Pfeiffer Vacuum) quadrupole mass spectrometer was used to analyze the gas phase composition. Calibration was carried out with mixtures of known gas composition. The following peaks were controlled simultaneously by the mass spectrometer: 4 (He), 18 (H_2O), 28 (N_2, N_2O), 30 (NO, N_2O), 32 (O_2), 40 (Ar), 44 (N_2O), and 46 (NO_2) m/e. The lines in the setup as well as a fused silica capillary connected to the mass spectrometer were heated up to 383–423 K.

The amount of catalyst placed in a quartz plug-flow reactor was equal to 1.04–1.09 g. Before every run the activated catalysts were pretreated in He (50 mL/min) at 1323 K for 1 h, then cooled to the studied temperature (523, 603, or 653 K). This pretreatment is hereafter called "standard."

In the transient response experiments a mixture of 2 vol% N_2O/2 vol% Ar/96 vol% He was introduced into the reactor at a flow rate of 20 mL(STP)/min. Argon was used as an inert tracer. Interaction of NO with the catalyst was studied with a mixture of 10 vol% NO/90 vol% Ar. After the N_2O or NO reacted with the catalyst, the reactor was purged with He for 10 min, and temperature-programmed desorption (TPD) was performed in He (20 mL/min) with a 30 K/min ramp.

All gases were obtained from CarbaGas (Lausanne) and had a purity higher than 99.998 vol%. Medical-grade N_2O (NO_x lower than 2 ppm) and pure N_2O (> 99.998%) were used. Water was pulsed to the catalyst using a 0.5-μL syringe via an injector. Adsorption of water was controlled by the mass spectrometer.

3. Results

3.1. Dynamics of N_2O decomposition

The transient response experiment with the HZSM-5$_{1000Fe}$ catalyst at 603 K is presented in Fig. 1 and illustrates the formation of N_2 and O_2. N_2 concentration first passes a sharp maximum and then slowly increases, while oxygen concentration is seen to continuously increase. After 45 min of reaction a steady state is reached with a conversion of around 50%. Nitrous oxide evolution is delayed with respect to Ar (inert tracer) due to product formation and reversible adsorption on the catalyst surface [13].

The HZSM-5$_{200Fe}$ catalyst behaves in a similar way at 603 an 653 K (Fig. 2). Two steps can be suggested to explain the dynamics of N_2O decomposition. The first is assigned to the formation of surface atomic oxygen $(O)_{ad}$ and gaseous N_2 from N_2O:
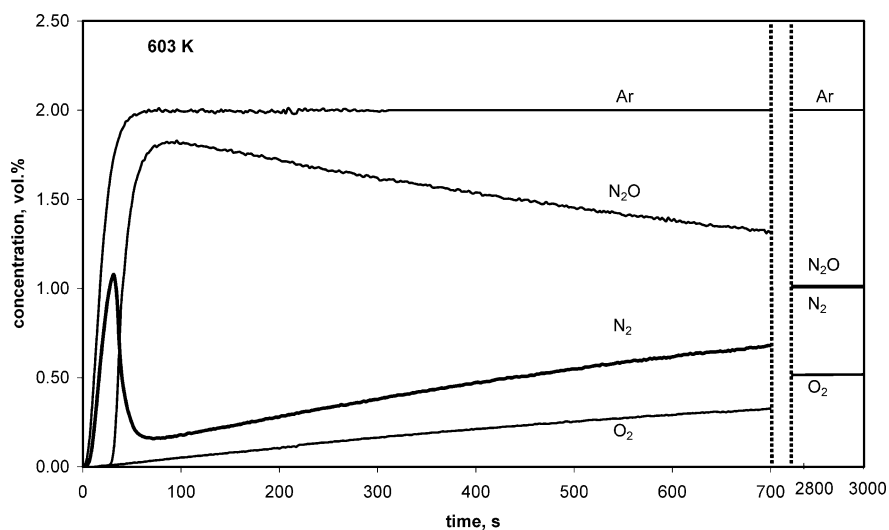
$$N_2O + (\ ) \rightarrow N_2 + (O)_{ads}.$$
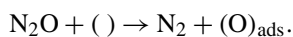
Fig. 1. Transient response curves obtained after introduction of the mixture of 2 vol.% N_2O/2 vol.% Ar in He on the HZSM-5$_{1000Fe}$ catalyst at 603 K after the standard pretreatment.
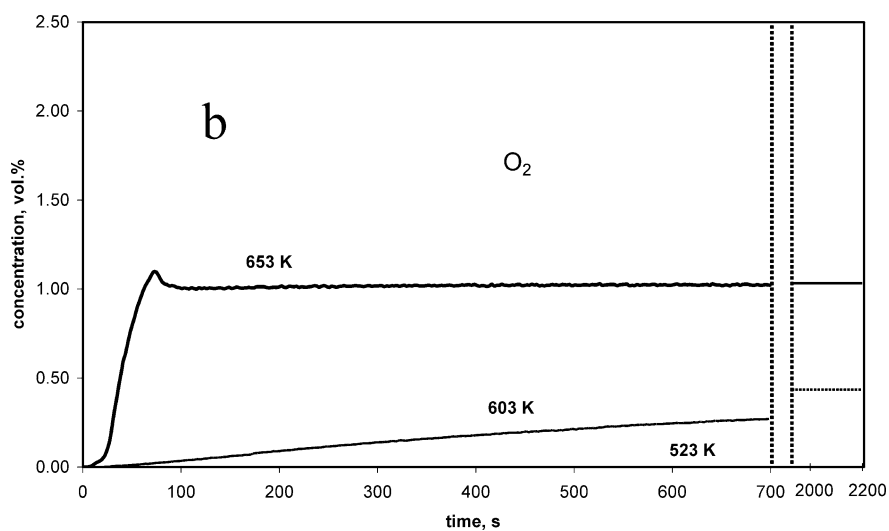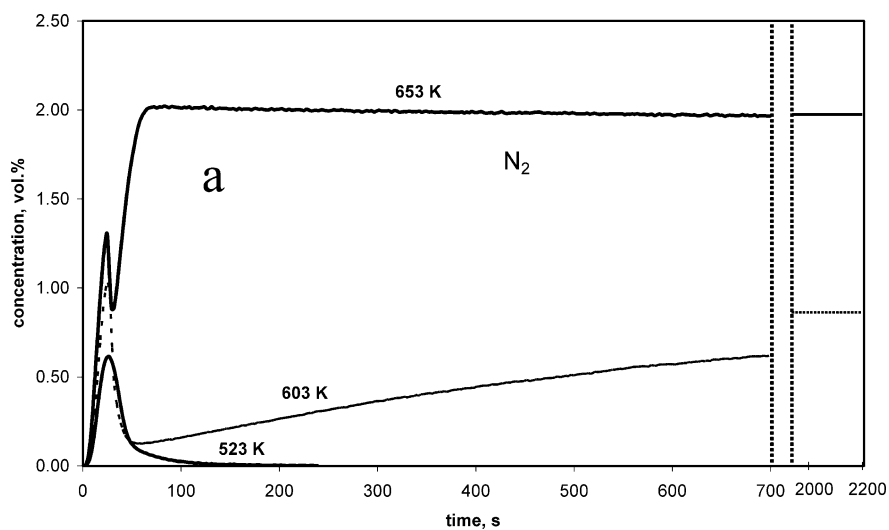
Fig. 2. Transient response curves of nitrogen (a) and oxygen (b) obtained after introduction of the mixture of 2 vol.% N_2O/2 vol.% Ar in He on HZSM-5$_{200Fe}$ catalyst at different temperatures after the standard pretreatment.
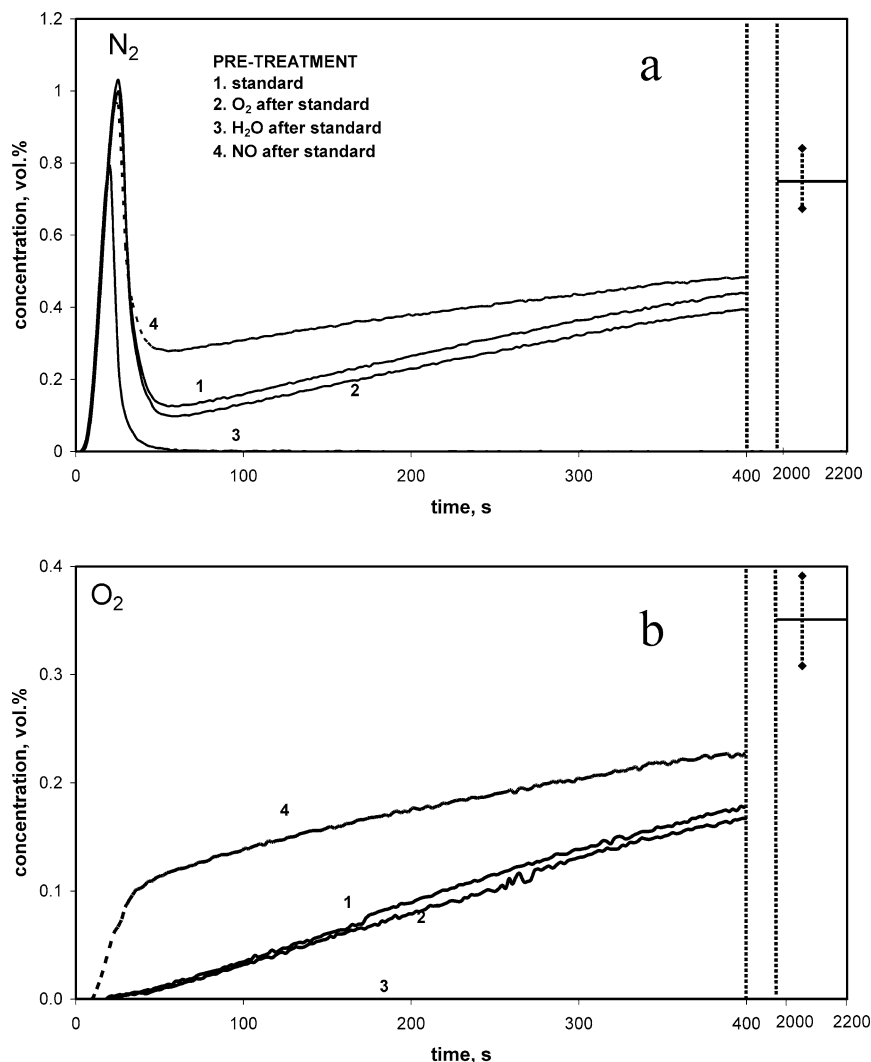
Fig. 3. Effect of the different pretreatments on the transient response curves of nitrogen (a) and oxygen (b) obtained after introduction of the mixture of 2 vol.% N_2O/2 vol.% Ar in He on HZSM-5$_{200Fe}$ catalyst at 603 K after the standard pretreatment (1, standard), followed by 2 vol% O_2 in He for 10 min (2, O_2), or water vapor (3, H_2O), or 10 vol% NO in Ar for 10 min (4, NO). A 10-min purge with He is performed after every pretreatment.

Only this reaction takes place at 523 K (Fig. 2). The N_2 appears in the reactor outlet with a sharp maximum, while the formation of molecular oxygen is not observed.

The second step during N_2O decomposition is characterized by a slow increase in O_2 concentration accompanied by N_2 formation in the stoichiometric ratio (Figs. 1–3). At higher temperature (653 K) the conversion rapidly reaches 100%.

It is important that the amount of nitrogen at 603 and 653 K determined by integration of the N_2 peak subtracting the nitrogen formed during the N_2O stoichiometric decomposition is equal to the amount of nitrogen evolved at 523 K. This was observed for both catalysts. Hence, the oxygen $(O)_{ad}$ deposited from N_2O occupies all surface Fe-active sites. The concentration of Fe-active sites for HZSM-5$_{200Fe}$ was found to be $(1.7 \pm 0.2) \times 10^{18}$ sites/g, which was calculated from the amount of N_2 released at 523 K. The concentration of active sites determined approaches the total

concentration of Fe atoms in the sample equal to 2.1×10^{18} atoms/g. However, for the HZSM-5$_{1000Fe}$ sample the concentration of active sites $((2.5 \pm 0.2) \times 10^{18}$ sites/g), is considerably lower than the total concentration of iron in the catalyst (1.1×10^{19} atoms/g).

3.2. Effect of catalyst pretreatments on N_2O decomposition dynamics

The dynamics of N_2O decomposition over the catalyst after standard pretreatment (1) was compared with those where the same pretreatment was followed by pretreatments in different gases at 603 K: (2) 2 vol% O_2 in He for 10 min (O_2); (3) water vapor until catalyst saturation with irreversibly adsorbed water (H_2O); (4) 10 vol% NO in Ar for 10 min (NO). It should be mentioned that after every pretreatment a 10-min He purge is performed.

It is seen in Fig. 3 that $(O)_{ad}$ formation on the surface is dependent on the type of pretreatment since the amount
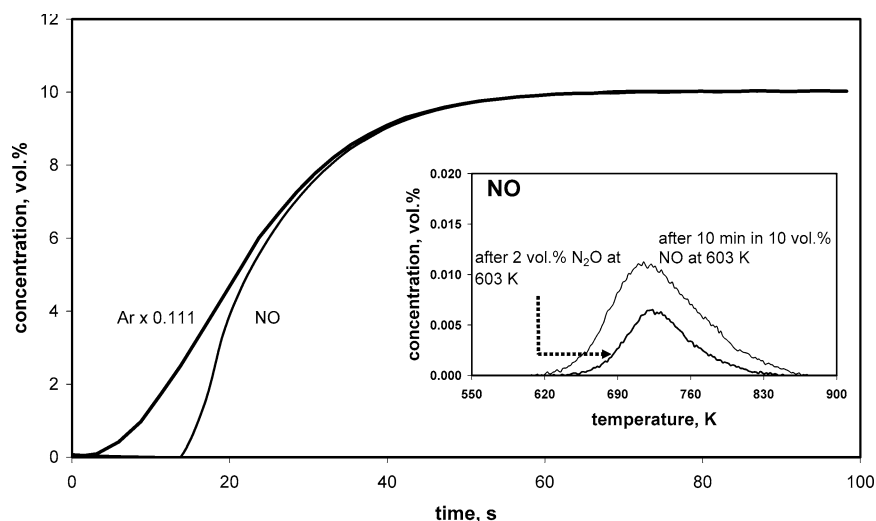
Fig. 4. Transient response curves obtained after a switch of He to the 10 vol% NO rest Ar mixture on HZSM-5$_{200Fe}$ at 603 K after the standard pretreatment. Inset: TPD profiles after interaction of NO and N$_2$O with HZSM-5$_{200Fe}$ at 603 K.

found from the nitrogen formed (after subtraction of the small contribution of N$_2$ formed during the stoichiometric decomposition of N$_2$O) was 1.7, 1.6, 0.8, and 1.3 × 10^{18} atoms/g after pretreatments 1, 2, 3, and 4, respectively.

Pretreatment with oxygen did not affect (O)$_{ad}$ loading and N$_2$O decomposition (Fig. 3). This result is in agreement with previous studies [8,10,13]. In contrast, water adsorption provided a twofold decrease in the amount of sites available for (O)$_{ad}$ formation. The same result for both catalysts studied was obtained at a lower temperature (523 K) [13]. Atomic surface oxygen recombination and desorption were more sensitive to pretreatment and were completely suppressed in the case of the H$_2$O-pretreated catalyst (Fig. 3). Additionally, catalyst presaturation with water considerably decreased (3.5–4 times) the amount of reversibly adsorbed N$_2$O as determined from the N balance. The N$_2$O adsorption was supposed to take place on Lewis acid sites [14], Fe^{2+}-sites, and Brønsted protons [15].

The result obtained for the effect of H$_2$O agrees with literature data. A decrease in N$_2$O conversion to N$_2$ and O$_2$ over Fe/MFI zeolites at 773 K after the introduction of water vapor has been reported [4,10].

The NO pretreatment turned out to have a very significant effect on the dynamics of N$_2$O decomposition (Fig. 3). The concentration of active sites participating in (O)$_{ad}$ formation after pretreatment decreased only ∼24% as compared with that for pretreatment in water vapor (∼50% decrease). The main effect of NO pretreatment was immediate initiation of O$_2$ release (O$_2$ response, Fig. 3). Roughly the same steady-state conversion (±10%) is reached as after the standard pretreatment. This indicates that some intermediates are left on the surface after NO pretreatment promoting this reaction. To check this, interaction of the 10 vol% NO/Ar mixture with the catalyst at 603 K was carried out and the results are shown in Fig. 4.

3.3. NO effects on decomposition of N$_2$O

The transient response with the NO-containing mixture is presented in Fig. 4, which shows a delay in NO evolution with respect to Ar. At the same time no gaseous products (O$_2$, N$_2$, NO$_2$, N$_2$O) were observed. The delay is explained by the adsorption of NO on the catalyst as no delay in the evolution of NO with respect to Ar was observed in a blank experiment with quartz instead of catalyst. The concentration of adsorbed NO was calculated to be 2.4 × 10^{18} molecules NO/g.

Temperature-programmed desorption (TPD) experiments indicated that even after the He purge, there remains on the surface some irreversibly adsorbed NO, which is desorbed at around 720 K (Fig. 4, inset). However, the amount of desorbed NO during TPD was more than one order of magnitude lower than the amount determined in the adsorption experiment (Fig. 4), indicating that the major portion of adsorbed NO was removed during the He purge.

It is important to note that NO evolution was also observed in the TPD experiment after N$_2$O decomposition (Fig. 4, inset). This result explains the dynamics of N$_2$O decomposition (Figs. 1, 2) and the effect of NO pretreatment on N$_2$O decomposition (Fig. 3). The same position of the TPD peak (Fig. 4, inset) suggests that the same surface species are formed during N$_2$O decomposition (Figs. 1–3) and during NO adsorption (Fig. 4). The adsorbed NO formed during N$_2$O interaction with the catalyst cannot be assigned to the impurities of NO (the level of < 2 ppm) in the N$_2$O gas. Hence, it was concluded that the adsorbed NO is formed in a trace amount from N$_2$O during its interaction with the catalyst.

The results obtained are in line with recent FTIR spectroscopy data [16] where the formation of adsorbed nitrosyl groups was observed during interaction of N$_2$O with Fe-ZSM-5 and Fe-MCM-41 at room temperature and as-
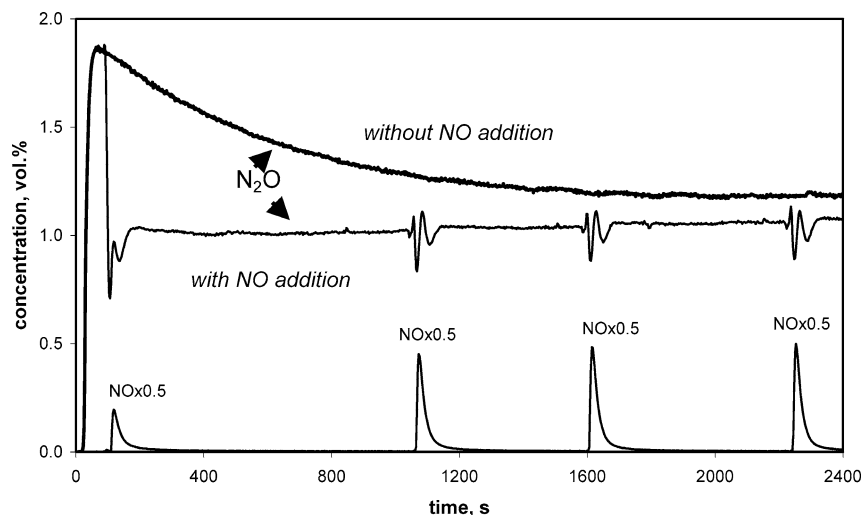
Fig. 5. Effect of NO pulse introduction on the N_2O response curve during interaction of the mixture of 2 vol.% N_2O/2 vol.% Ar in He with HZSM-5$_{200Fe}$ at 603 K.

cribed to

$$N_2O \rightarrow NO_{ads} + 0.5N_2.$$

Formation of NO from N_2O has been also taken into account in [4,10] as a possible step in NO_x group formation from N_2O. NO evolution was observed in TPD profiles after interaction of N_2O with different zeolites containing iron [4,17], and copper [18] and with some other catalysts [17].

The promoting effect of NO on N_2O decomposition over Fe-ZSM-5 zeolites is well known [6,11,19]. To study the effect of NO on the dynamics of N_2O decomposition over HZSM-5$_{200Fe}$, the reaction mixture (2 vol% N_2O/2 vol% Ar/He) was periodically passed through a 2-mL loop filled with a 10 vol% NO/Ar mixture. It is seen in Fig. 5 that after introduction of the first NO pulse, the steady-state N_2O decomposition was immediately attained, which is not the case for the run without NO (Fig. 5). The following NO pulses do not disturb the steady state. The same steady-state conversion is reached with and without forced NO doping. Formation of negligible amounts of NO_2 (< 0.01 vol%) during the NO pulse was observed. These data indicate that introduction of NO results in the rapid formation of surface species leading to steady-state N_2O decomposition. Their surface concentration (1.7×10^{18} molecules NO/g) almost does not change after the first NO pulse.

The NO promotion mechanism was considered by Moulijn et al. [6,11] and Sang and Lund [19,20]. The catalytic effect of NO could be explained by: (1) scavenging of surface atomic oxygen by gaseous NO giving NO_2 similarly to CO and regenerating active sites for interaction with N_2O; (2) facilitation of molecular oxygen formation and desorption due to the adsorbed NO [6] or NO_x [19,20] species.
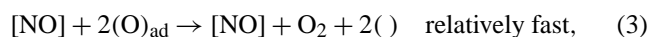
No NO_2 was found during the reaction under the conditions reported in Figs. 1–3. This means that the first mechanism of NO promotion may not be important, espe-

cially taking into account the small amount of NO formed during N_2O interaction with the catalyst.

The TPD data after different exposures of the catalyst to N_2O at 523 K reveal an increase in strongly adsorbed NO with time (Figs. 6b, 7). It is important that at the same time, the O_2 peak shifts to lower temperatures, confirming the catalytic role of adsorbed NO. Small amounts of NO result in a 60 K shift in temperature for the maximal rate of O_2 desorption (Figs. 6a, 7 inset), but the amount of oxygen in the TPD peak seems to be independent of the adsorbed NO concentration (Fig. 7). Thus, irreversibly adsorbed NO formed during N_2O decomposition acts as a catalyst for N_2O decomposition. Also interesting is that irreversible adsorption of water at 523 K on the zeolite before N_2O decomposition was found to suppress NO formation on the surface as confirmed by TPD measurements (not shown).

4. Discussion

A reaction scheme is proposed to explain the experimental data:

$N_2O \leftrightarrow N_2O_{ad}$ (reversible adsorption),

$N_2O + (\ ) \rightarrow N_2 + (O)_{ad}$ fast,   (1)

$N_2O + [\ ] \rightarrow [NO] + 0.5N_2$ slow,   (2)

$[NO] + 2(O)_{ad} \rightarrow [NO] + O_2 + 2(\ )$ relatively fast,   (3)

$2(O)_{ad} \rightarrow O_2 + 2(\ )$ slow.   (4)

At 523 K only the first two steps seem to occur. The first step corresponds to surface atomic oxygen formation. Extraframework Fe^{2+} sites created by autoreduction of Fe^{3+} to Fe^{2+} during thermal treatment of the zeolite in He or vacuum [13,21–25] are suggested as the active sites for this reaction. NO is formed in the second step and accumulates slowly on the zeolite surface. It participates in the reaction as
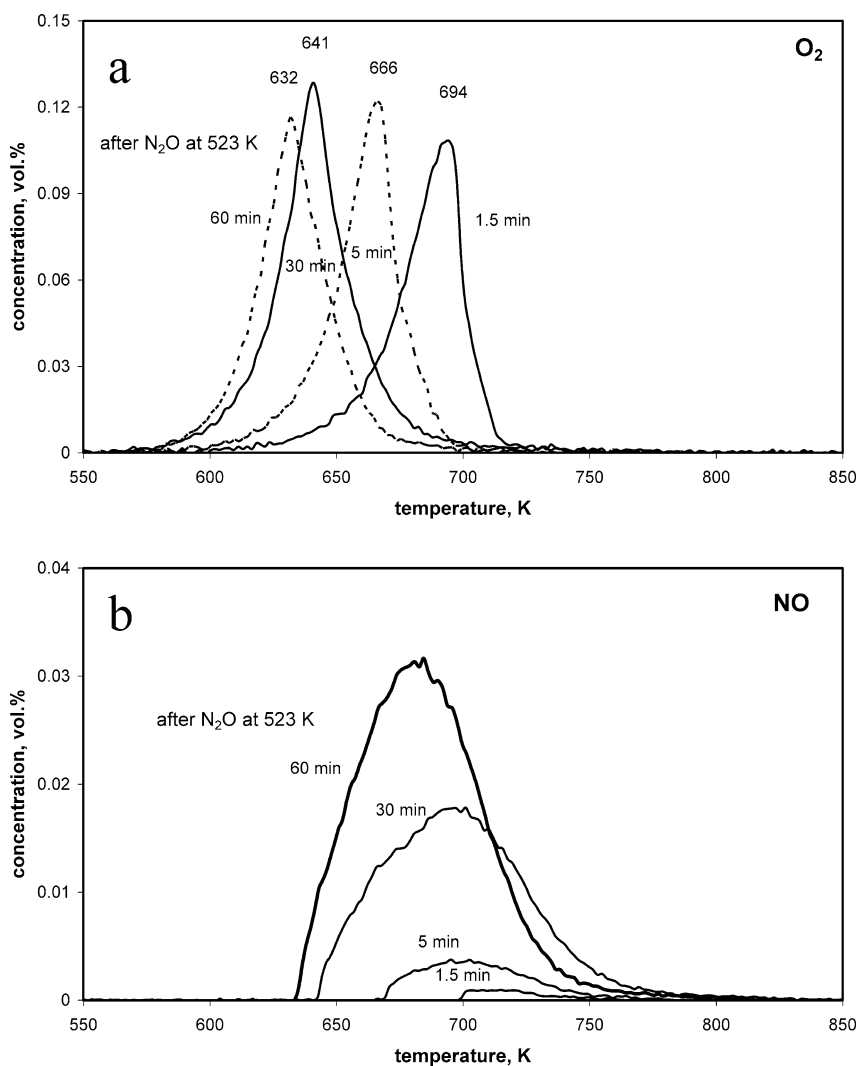
Fig. 6. Effect of exposure time of HZSM-5$_{200Fe}$ in the mixture of 2 vol.% N$_2$O/2 vol.% Ar in He at 523 K on the TPD profiles of O$_2$ (a) and NO (b).
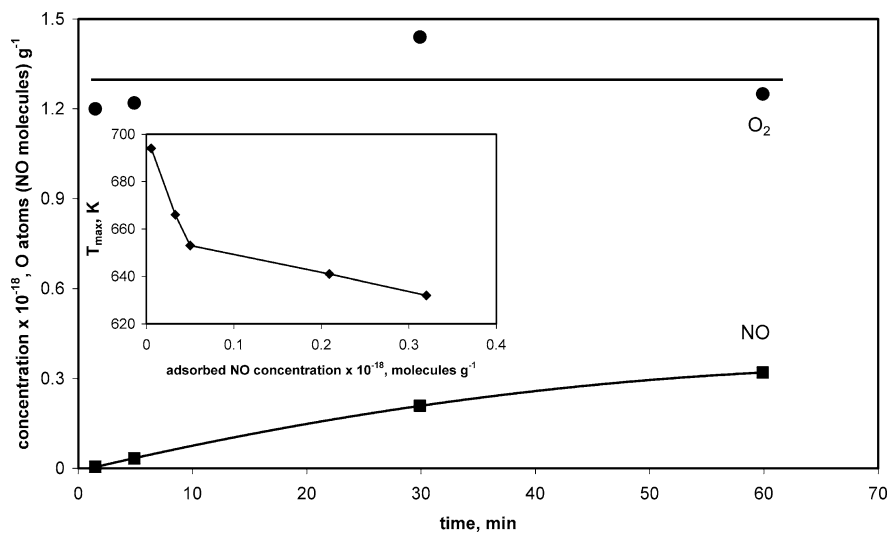

Fig. 7. Concentrations of O$_2$ and NO desorbed in TPD runs after exposure of HZSM-5$_{200Fe}$ to the mixture of 2 vol.% N$_2$O/2 vol.% Ar in He for different times. Inset: Dependence of the temperature of maximal rate of O$_2$ desorption on the concentration of irreversibly adsorbed NO.

a catalyst, increasing the oxygen recombination and desorption rate (step 3). That the adsorbed NO accumulates on the surface in time even when all iron sites are covered by oxygen via interaction with N_2O at 523 K is significant (Fig. 7). Hence, different sites are suggested for the formation of adsorbed [NO] and $(O)_{ad}$ deposition from N_2O.

Step 4 is considered in the literature as completing the catalytic cycle during N_2O decomposition [21]. However, the increase in N_2O decomposition rate and reaction dynamics (Figs. 1–3) may not be explained in the framework of steps 1 and 4 without considering catalysis by [NO]. To make the interaction of adsorbed NO with adsorbed oxygen feasible, these two species should be present in close proximity. This is possible if the Fe site is not isolated, but binuclear [13,21] or oligonuclear [26]. In accordance, N_2O decomposition activity over a Fe silicalite containing isolated iron sites was shown to be much lower than that over Fe-AlZSM-5 containing oligonuclear Fe sites [26].

Water vapor influences drastically the active sites for surface oxygen loading. They can adsorb only half the amount of oxygen from N_2O as compared with the dry conditions (Fig. 3). Moreover, oxygen desorption takes place at temperatures several hundred degrees higher [13]. According to FT-IR spectroscopy studies of the hydroxyl group region, Zhu et al. [27] suggested that on water treatment at 823 K cationic Fe species agglomerate and transform into Fe oxide species. Further work seems to be necessary to follow the iron species transformations during these reactions.

5. Conclusions

1. N_2O decomposition over isomorphously substituted H(Fe)ZSM-5 was studied by the transient response method. The catalysts were activated by steaming at 823 K followed by thermal treatment in He at 1323 K.
2. Two steps were distinguished from the reaction dynamics: (1) a fast surface atomic oxygen deposition from N_2O with gaseous nitrogen release, and (2) a slow atomic oxygen recombination/desorption (the rate-limiting step).
3. Oxygen recombination/desorption was observed to be accelerated by small amounts of irreversibly adsorbed NO slowly formed and accumulated on the catalyst surface during N_2O decomposition as confirmed by TPD. The slow accumulation of NO results in a slow increase in the rate of N_2O decomposition with time.
4. A simplified kinetic model is proposed to explain the autocatalytic reaction. Adsorbed NO is formed on sites different from those for atomic oxygen deposition from N_2O.
5. Catalyst pretreatment with oxygen does not influence N_2O decomposition. Irreversibly adsorbed water sup-

presses the oxygen recombination/desorption step, rendering the zeolite catalyst inactive toward N_2O decomposition.

Note added in proof. Very recently Pirngruber [28] also observed, by the transient response method, the two-step behavior during N_2O decomposition, with oxygen desorption being the rate-limiting step, although the zeolites used in his study contained much higher concentrations of iron ($> 26,000$ ppm).

References

[1] W.C. Trogler, Coord. Chem. Rev. 187 (1999) 303.
[2] F. Kapteijn, J. Rodriguez Mirasol, J.A. Moulijn, Appl. Catal. B 9 (1996) 25.
[3] V.I. Sobolev, G.I. Panov, A.S. Kharitonov, V.N. Romannikov, A.M. Volodin, K.G. Ione, J. Catal. 139 (1993) 435.
[4] E.M. El-Malki, R.A. van Santen, W.M.H. Sachtler, J. Catal. 196 (2000) 212.
[5] Q. Zhu, B.L. Mojet, R.A.J. Janssen, E.J.M. Hensen, J. van Grondelle, P. Magusin, R.A. van Santen, Catal. Lett. 81 (2002) 205.
[6] J. Perez-Ramirez, F. Kapteijn, G. Mul, J.A. Moulijn, J. Catal. 208 (2002) 211.
[7] K.A. Dubkov, V.I. Sobolev, E.P. Talsi, M.A. Rodkin, N.H. Watkins, A.A. Shteinman, G.I. Panov, J. Mol. Catal. A 123 (1997) 155.
[8] G.I. Panov, A.K. Uriarte, M.A. Rodkin, V.I. Sobolev, Catal. Today 41 (1998) 365.
[9] B. Louis, L. Kiwi-Minsker, P. Reuse, A. Renken, Ind. Eng. Chem. Res. 40 (2001) 1454.
[10] E.M. El-Malki, R.A. van Santen, W.M.H. Sachtler, Micropor. Mesopor. Mater. 35-6 (2000) 235.
[11] G. Mul, J. Perez-Ramirez, F. Kapteijn, J.A. Moulijn, Catal. Lett. 77 (2001) 7.
[12] T. Turek, J. Catal. 174 (1998) 98.
[13] L. Kiwi-Minsker, D.A. Bulushev, A. Renken, J. Catal. 219 (2003) 273.
[14] V.M. Mastikhin, Colloid Surf. A 78 (1993) 143.
[15] B.R. Wood, J.A. Reimer, A.G. Bell, J. Catal. 209 (2002) 151.
[16] G. Grubert, M.J. Hudson, R.W. Joyner, M. Stockenhuber, J. Catal. 196 (2000) 126.
[17] M. Mauvezin, G. Delahay, B. Coq, S. Kieger, J.C. Jumas, J. Olivier-Fourcade, J. Phys. Chem. B 105 (2001) 928.
[18] M. Shimokawabe, K. Hirano, N. Takezawa, Catal. Today 45 (1998) 117.
[19] C.M. Sang, C.R.F. Lund, Catal. Lett. 73 (2001) 73.
[20] C.M. Sang, C.R.F. Lund, Catal. Lett. 70 (2000) 165.
[21] K.A. Dubkov, N.S. Ovanesyan, A.A. Shteinman, E.V. Starokon, G.I. Panov, J. Catal. 207 (2002) 341.
[22] G. Berlier, G. Spoto, P. Fisicaro, S. Bordiga, A. Zecchina, E. Giamello, C. Lamberti, Microchem. J. 71 (2002) 101.
[23] P. Kubanek, B. Wichterlova, Z. Sobalik, J. Catal. 211 (2002) 109.
[24] A.L. Yakovlev, G.M. Zhidomirov, R.A. van Santen, J. Phys. Chem. B 105 (2001) 12297.
[25] J. Jia, B. Wen, W.M.H. Sachtler, J. Catal. 210 (2002) 453.
[26] J. Perez-Ramirez, F. Kapteijn, A. Bruckner, J. Catal. 218 (2003) 234.
[27] Q. Zhu, E.J.M. Hensen, B.L. Mojet, J. van Wolput, R.A. van Santen, Chem. Commun. (2002) 1232.
[28] G.D. Pirngruber, J. Catal. 219 (2003) 456.